

- (4) Cantera, F. B.; Riande, E.; Almendro, J. P.; Saiz, E. *Macromolecules* **1981**, *14*, 138.
- (5) Saiz, E.; Riande, E.; Delgado, M.; Barrales-Rienda, J. M. *Macromolecules* **1982**, *15*, 1152.
- (6) Marchal, J.; Benoit, H. *J. Chim. Phys. Phys.-Chim. Biol.* **1955**, *52*, 818.
- (7) Marchal, J.; Benoit, H. *J. Polym. Sci.* **1957**, *23*, 223.
- (8) Stockmayer, W. H. *Pure Appl. Chem.* **1967**, *15*, 539.
- (9) Nagai, K.; Ishikawa, T. *Polym. J.* **1971**, *2*, 416.
- (10) Doi, M. *Polym. J.* **1972**, *3*, 252.
- (11) Abe, A.; Jernigan, R. L.; Flory, P. J. *J. Am. Chem. Soc.* **1966**, *88*, 631.
- (12) Flory, P. J. *Macromolecules* **1974**, *7*, 381.
- (13) Mattice, W. L. *Macromolecules* **1981**, *14*, 1485.
- (14) Mattice, W. L. *Macromolecules* **1981**, *14*, 1491.

Dielectric Relaxation of Oxide Polymers in Dilute Solution[†]

Satoru Mashimo* and Shin Yagihara

Department of Physics, Tokai University, Hiratsuka-shi, Kanagawa 259-12, Japan

Akio Chiba

Department of Applied Physics, Waseda University, Shinjuku-ku, Tokyo 160, Japan.

Received August 29, 1983

ABSTRACT: Dielectric relaxation measurements were made on dilute solutions of poly(propylene oxides) in benzene over a wide frequency range from 10 MHz to 10 GHz using time-domain reflectometry. Two relaxation processes were found. The lower frequency process, depending strongly on the molecular weight, is explained completely by the normal mode theory of Rouse and Zimm. Another process, independent of molecular weight, is caused by an elementary process in the backbone motion. The magnitude of the relaxation time is explained satisfactorily by Kramers' rate constant theory at the low-friction limit, if the elementary process is assumed to be a rotational transition of a chain bond. The relaxation process observed in poly(ethylene oxide) in benzene is also explained by Kramers' theory. The effect of chemical structure of oxide polymers on the higher frequency relaxation process is discussed.

I. Introduction

Three kinds of dielectric relaxation processes have been found in solutions of flexible polar polymers. If a polymer has dipole components parallel to its chain contour, a rotational diffusion of the polymer molecule gives rise to a relaxation process depending on molecular weight in a relatively low frequency region.¹ The relaxation time is explained quite satisfactorily by the normal mode theory of Rouse and Zimm.^{2,3} The theory predicts relaxation time as

$$\tau_{\text{rot}} = A_1 M [\eta] \eta_0 / RT \quad (1)$$

where M is the molecular weight, $[\eta]$ the intrinsic viscosity, η_0 the solvent viscosity, R the gas constant, and T the absolute temperature. The factor A_1 takes a value of 1.21 for the free-draining case and 0.85 for the nondraining case. Poly(ϵ -caprolactone) (PCL) and poly(olefin sulfones) in solution exhibit this relaxation process.⁴⁻⁶

Generally, polar polymers have dipole components perpendicular to the chain contour and show a relaxation process independent of molecular weight which is observed in a relatively high frequency region.^{1,7-9} Chain motions associated with conformational transitions in the chain backbone give rise to this relaxation. Recent study of methyl methacrylate-methyl acrylate copolymers in dilute solution has indicated that the elementary process in the chain motion is essentially a bond rotation which occurs independently between isomeric transition states.¹⁰

Poly(*p*-chlorostyrene) is a typical polymer having a dipole component of this type. The relaxation peak was found at about 30 MHz in solution.⁷⁻⁹ The relaxation time is expressed experimentally by⁷

$$\tau_{\text{back}} = A_2 \eta_0 \exp(\Delta H_A / RT) \quad (2)$$

This expression is explained quite satisfactorily by Kramers' rate constant theory at the high-friction limit.^{11,12} The value of ΔH_A represents the potential barrier height for bond rotation. If correlated motions are assumed to exist among several neighboring bonds, the magnitude of the factor A_2 is explained by Kramers' theory.⁷

If the relaxation peak is found at a frequency lower than 100 MHz, the same argument can hold well for other polar polymers such as vinyl polymers^{7,8} and poly(alkyl methacrylates)¹³ in dilute solution.

Recently, a relaxation caused by internal rotations of side groups has been found in poly(methyl vinyl ketone) in benzene.¹⁵ Rotation of acetyl side groups gives a relaxation peak at 1 GHz. Relaxation of this kind in the solid state is observed in a number of polymers. This result indicates that relaxation caused by side-group rotation exists even in a dilute polymer solution.

If a polymer contains oxygen atoms in the chain backbone, as in the polyethers, a dielectric relaxation peak occurs at a very high frequency. Poly(ethylene oxide) (PEO) exhibits a peak at about 10 GHz in benzene,¹⁶ and PCL has one at 2 GHz in dioxane.^{4,17} Poly(styrene oxide) (PSO) shows a peak at 450 MHz in benzene, which is about 5 times higher than that of polystyrene.¹⁸

Most likely, the backbone motions in these polymers also cause the relaxation observed. Therefore, it is thought to be quite important in interpreting chain dynamics to examine whether Kramers' rate constant at the high-friction limit can or cannot be applied to the relaxation times of these polymers as well as of vinyl polymers and to determine why the relaxation time is very small in comparison with other polar polymers.

In this work poly(propylene oxides) with different molecular weights were used as the polymer having oxygen atoms in the chain backbone, and dielectric relaxation

[†] This paper is dedicated, with great pleasure and appreciation, to Professor Walter H. Stockmayer on the occasion of his 70th birthday celebration.

measurements were made on dilute solutions in benzene over a wide frequency range extending from 10 MHz to 10 GHz using the time-domain reflectometry (TDR) method.^{17,19-21}

Poly(propylene oxide) (PPO) has two types of dipole components.^{1,22} One is parallel to the chain contour and the other perpendicular to the contour. Therefore two kinds of relaxation processes are expected to be observed in its dilute solution. Previously, Baur and Stockmayer found two relaxation processes in liquid PPO. One is the process depending on molecular weight and the other is caused by the backbone motions.²²

Dielectric relaxation measurements were also made on PEO in benzene using the TDR method in order to ascertain the relaxation mechanism for oxide polymers in dilute solution.

II. Experimental Section

Four samples of PPO, viscosity-average molecular weights of which are 440, 700, 1160, and 2020, respectively, were provided by Sekisui Chemical Co. Ltd. A sample of PPO with a molecular weight M of 3000 was obtained from Asahi Denka Industry and a sample with $M = 4000$ was obtained from General Science Corp. Gel permeation chromatography (GPC) measurements indicated that these samples had fairly narrow molecular weight distributions. The ratio of \bar{M}_w/\bar{M}_n is less than 1.1.

A sample of PEO with $M = 4.0 \times 10^4$ was used as a standard sample for GPC measurements. It was obtained from Toyo Soda Manufacturing Co. Ltd.

The TDR apparatus employed was similar to those reported previously.^{20,21} In this work, a sampling scope (Iwatsu Electric SAS-601B, DC-12.4GHz) and two sampling heads (Iwatsu Electric SH-4B, DC-12.4GHz) were used. A signal analyzer (Iwatsu Electric SM-2100A) was used as a transient recorder.

The method of making measurements is an improved difference method,¹⁷ which is very useful for measurement of a small difference between permittivity ϵ_x of a dilute polymer solution and permittivity ϵ_s of the reference solvent. The relation between these quantities at a circular frequency ω is

$$\epsilon_x = \epsilon_s \frac{1 + gh}{1 - i\omega[\gamma d \epsilon_s / cf(z_s)]gh} \frac{f(z_x)}{f(z_s)}$$

$$g = \frac{r_s - r_x}{r_a - r_s}$$

and

$$h = \frac{1 - f(z_s)/\epsilon_s f(z_a)}{1 + i\omega\gamma d/cf(z_a)} \quad (3)$$

where r_a , r_s , and r_x are the Laplace transforms of the pulse reflected from air, from the solvent, and from the solution, respectively, d is the length of the cylindrical central conductor of the sample cell, γd is the effective length of the conductor, and c is the speed of propagation in vacuo (0.300 mm/ps).

The function $f(z)$ is given by

$$f(z) = z \cot z \quad (4)$$

where $z = (\omega d/c)\epsilon^{1/2}$ accounts for propagation and multiple reflections in the sample. Equation 4 places a definite restriction on the choice of cell length, because $f(z)$ diverges at $|z| = \pi/2$, and hence eq 3 is useful for $|z| < 1$. Further, if the effective cell length γd is chosen so that $\gamma d \epsilon_s/c$ is much less than the relaxation time τ of the solution measured, dispersion and absorption can be measured easily and accurately.²¹ Therefore we chose a cell (cell 1) with $d = 5.0$ mm and $\gamma d = 15.93$ mm for measurements from 10 MHz to 2 GHz and a very short cell (cell 2) with $d \leq 0.05$ mm and $\gamma d = 0.506$ mm for use in the range 0.1–10 GHz. The length of the short cell could not be determined accurately. However, it is likely that $f(z)$ takes a value of unity at frequencies up to 20 GHz for the samples in this work. It is expected that a relaxation process with a very short relaxation time of approximately 5 ps can be measured accurately with this short cell.

In order to examine the adequacy of the cell length for the present measurements, toluene was measured as a test sample,

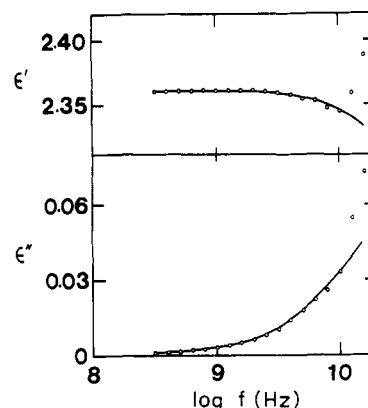


Figure 1. Dielectric dispersion and absorption for toluene at 23 °C using short cell 1 and benzene as a reference sample. Solid curves are the best fitted curves calculated from the Debye representation.

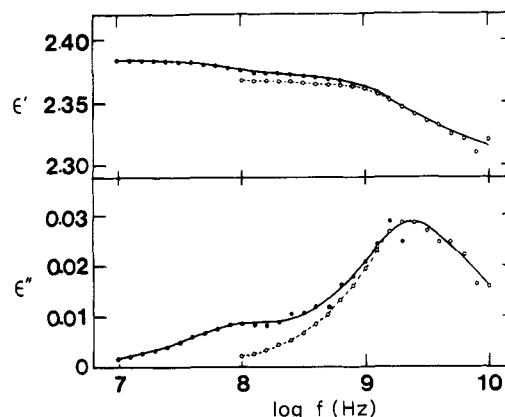


Figure 2. Dielectric dispersion and absorption for 5% (w/w) PPO with $M = 4000$ in benzene at 25 °C using cell 1 (●) and cell 2 (○). Solid curves are those calculated from eq 6. Dotted curves are those calculated for the higher frequency relaxation using the parameters listed in Table I.

with benzene as a reference. The results are shown in Figure 1. Toluene has a Debye relaxation with a relaxation time of about 7 ps and an increment of about 0.1 at 20 °C. Solid curves shown in Figure 1 are calculated curves best fitted to the experimental data. The relaxation time obtained from the curves is 6 ps and the increment is 0.100. Furthermore, the ϵ_0 of toluene is also a reasonable value of 2.361.

Figure 1 indicates that the highest frequency attainable by this TDR method is about 10 GHz. This limit may result from the frequency limit of the sampling scope, which is 12.4 GHz.

III. Experimental Results

Dispersion and absorption curves for a 5.0% (w/w) solution of PPO with $M = 4000$ in benzene at 25 °C are shown in Figure 2. The difference between results obtained with the different cells is negligible over the frequency range 1–2 GHz. Absorption curves of other PPO solutions at 25 °C are shown in Figure 3.

As is seen in Figures 2 and 3, two relaxation processes were found in PPO with a molecular weight higher than 2020. The lower frequency process shifts to a higher frequency region as the molecular weight decreases. In the case of PPO with a molecular weight lower than 1160, two relaxation peaks merge into a single dispersion region.

For a quantitative treatment, the complex permittivity was assumed to be the sum of two Havriliak-Negami²³ contributions:

$$\epsilon_x = \epsilon_\infty + \frac{\Delta\epsilon_h}{[1 + (i\omega\tau)_h^{\beta_h}]^{\alpha_h}} + \frac{\Delta\epsilon_l}{[1 + (i\omega\tau)_l^{\beta_l}]^{\alpha_l}} \quad (5)$$

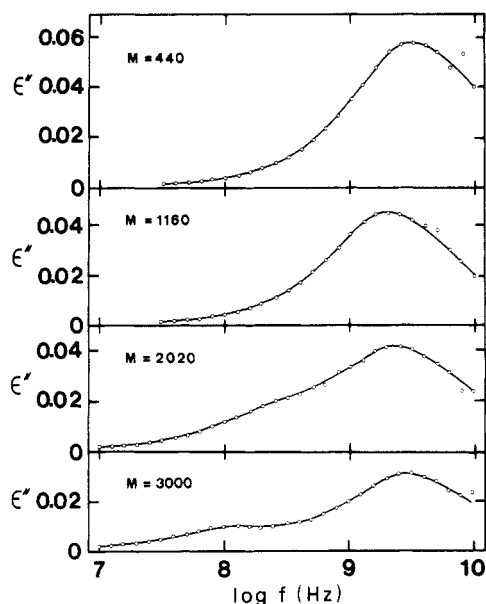


Figure 3. Dielectric absorptions of 5% (w/w) PPO in benzene at 25 °C. The solid curves are calculated from eq 6.

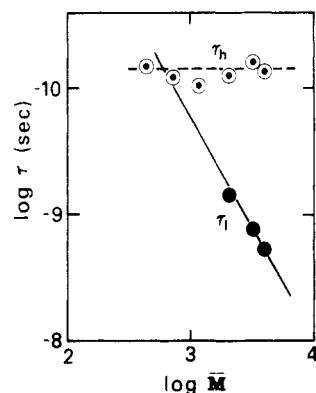


Figure 4. Plots of relaxation times τ_h and τ_1 for 5% PPO in benzene at 25 °C. The solid line is calculated from eq 10.

Table I
Parameters of Dielectric Relaxation of 5% (w/w)
PPO in Benzene at 25 °C

M	τ , ps	α	β	$\Delta\epsilon$	ϵ_∞	$\langle\mu^2\rangle^{1/2}$, D
Higher Frequency Dispersion						
440	67	0.70	1.00	0.137	2.322	
700	83	0.70	1.00	0.123	2.315	
1160	95	0.77	1.00	0.102	2.309	
2020	79	0.75	1.00	0.091	2.321	0.97
3000	62	0.78	1.00	0.068	2.291	0.85
4000	74	0.80	1.00	0.063	2.308	0.81
Lower Frequency Dispersion						
2020	700	1.00	1.00	0.022	2.412	0.47
3000	1500	1.00	1.00	0.014	2.369	0.38
4000	1900	1.00	1.00	0.013	2.371	0.36

Appropriate values of the parameters in eq 5 were chosen to give curves best fitted to the experimental dispersion and absorption results. Figures 2 and 3 completely confirm the adequacy of eq 5. Values of the parameters calculated by eq 5 are listed in Table I. The parameters $\alpha_h = 0.8$ and $\beta_h = 1.00$ mean that the higher frequency relaxation corresponds to the Cole–Davidson process, while $\alpha_1 = \beta_1 = 1.00$ means that the lower frequency process is a simple Debye relaxation.

The relaxation times τ_h and τ_1 are plotted against molecular weight in Figure 4. The relaxation time τ_1 is

Table II
Temperature Variation of Relaxation Parameters for
Higher Frequency Dispersion of 5% (w/w) PPO
with $M = 4000$ in Benzene

T , °C	τ_h , ps	α_h	β_h	$\Delta\epsilon$	ϵ_∞	ΔH_A , kcal/ mol
10.3	97	0.90	1.00	0.066	2.345	
20.0	90	0.85	1.00	0.065	2.336	2.7
25.0	74	0.80	1.00	0.063	2.308	
35.3	69	0.85	1.00	0.055	2.296	

Table III
Relaxation Parameters for PEO in Benzene at 20 °C

concn, % (w/w)	τ , ps	α	β	$\Delta\epsilon$	ϵ_∞	$\langle\mu^2\rangle^{1/2}$, D
5	19	1.00	0.80	0.155	2.337	1.08
10	17	1.00	0.84	0.280	2.344	1.02

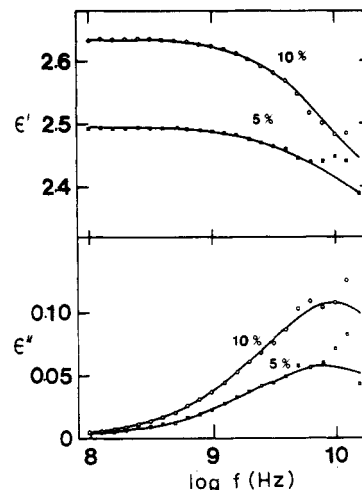


Figure 5. Dispersion and absorption for solutions of PEO in benzene at 20 °C. The solid curves are calculated from the Cole–Cole representation using parameters in Table III.

strongly dependent on molecular weight, while τ_h does not depend on it within experimental error. The only exception is PPO with $M = 1160$, where τ_h is a little larger. This may be due to the fact that the peak observed lies between two relaxation peaks.

When the shorter cell (cell 2) is used, only the higher frequency dispersion is observed, as is shown in Figure 2. Therefore in order to obtain an apparent activation energy for the higher frequency process, cell 2 was employed and measurements were made on a 5% (w/w) solution of PPO with $M = 4000$ in benzene at various temperatures. The results are given in Table II.

Effective mean square dipole moments per repeat unit calculated from the Onsager equation are listed in Table I. In the case where the molecular weight is 1160 or lower, two dispersions cannot be distinguished and hence the dipole moments cannot be obtained. The dipole moment for the higher frequency dispersion of PPO with the highest molecular weight ($M = 4000$) is 0.81 D. The dipole moment ratio $\langle\mu_h^2\rangle/\mu_0^2$ is 0.46, which is very close to the value predicted by a conformational energy analysis.²⁴ In this calculation, a value of 1.20 D was used as μ_0 .

In the case of PEO in benzene, a relaxation process was found as shown in Figure 5. The complex permittivities are described well by the Cole–Cole representation with $\beta = 0.80$ –0.84. The relaxation parameters listed in Table III are in good agreement with those reported previously.¹⁶ The effective dipole moment calculated is 1.02–1.08 D and is also in complete agreement with those reported.²⁵

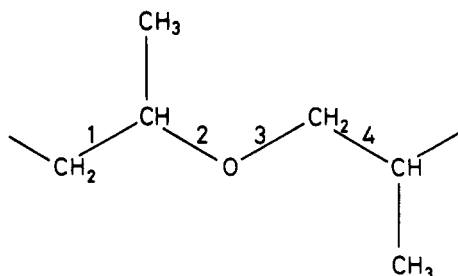


Figure 6. PPO chain.

IV. Discussion

1. Lower Frequency Dispersion of PPO. Previously, Baur and Stockmayer found in liquid PPO a relaxation depending on molecular weight and concluded that the free-draining formula of the normal mode theory for liquid polymer gives a satisfactory explanation of the relaxation time.^{1,22} However, in this case, PPO has two sequences of parallel components of dipoles pointing in opposite directions from a location near the middle of the chain contour. Therefore the mode with $k = 2$ is the dominant one. The relaxation time observed agrees well with that predicted by the theory of Bueche with $k = 2$.

This result suggests that the same argument holds well for the present PPO solution. In dilute solution, the free-draining formula of the normal mode theory with $k = 2$ is¹⁻³

$$\tau_1 = \tau_{\text{rot}}/k^2 = 0.303M[\eta]\eta_0/RT \quad (6)$$

For a benzene solution of PPO, $[\eta]$ obtained experimentally is

$$[\eta] = 11.1 \times 10^{-3} M^{0.79}, \quad 700 \leq M \leq 3300 \quad (7)$$

at 20 °C²⁶ and

$$[\eta] = 11.2 \times 10^{-3} M^{0.78}, \quad 3 \times 10^4 \leq M \leq 7 \times 10^5 \quad (8)$$

at 25 °C.²⁷ Substitution of eq 7 into eq 6 gives

$$\log \tau_1 = -15.17 + 1.79 \log M \quad (9)$$

at 20 °C. The solid line in Figure 4 is calculated from eq 9. It is clear that eq 9 gives a complete explanation for the lower frequency relaxation of PPO in benzene.

2. Higher Frequency Dispersion of PPO. In general, the potential barrier height for backbone motion is thought to be 2–3 kcal/mol.^{10,28} The activation energy of 2.7 kcal/mol for the higher frequency relaxation suggests that the activation energy corresponds to the barrier height for backbone motion, and Kramers' rate constant at the low-friction limit^{11,12} is applicable to the relaxation process.

Kramers' rate constant between isomeric transition states such as trans and gauche at the low-friction limit is

$$k_s = \frac{3}{4\pi} \left(\frac{E^*}{I} \right)^{1/2} \exp(-E^*/RT) \quad (10)$$

where I is the moment of inertia of the rotating unit around a chain bond and the threefold potential energy is assumed to have the form

$$U = \frac{1}{2} E^* (1 - \cos 3\vartheta) \quad (11)$$

In the PPO chain, four kinds of bond rotations are active in dielectric relaxation (see Figure 6). Rotation of O atom, H atom, and CH₃ groups around C–C bond 1 (rotation 1), that of a CH₂ group around C–O bond 2 (rotation 2), that of the CH(CH₃) group around C–O bond 3 (rotation 3), and that of an O atom and two H atoms around C–C bond 4 (rotation 4) are those rotations. The value of 2.7 kcal/mol observed for the activation energy is quite reasonable for

the potential barrier of these rotational transitions.²⁹

The rate constants of these transitions seem to differ from each other. A distribution of relaxation times may arise from this difference. However, the existence of correlated motions among neighboring bonds average out these different constants. A single-relaxation process is therefore observed. An average rate constant \bar{k} will give an approximate relaxation time

$$\tau_h \approx 1/\bar{k} \quad (12)$$

The moment of inertia of rotation 1 is 0.92×10^{-38} g cm². If the value of ΔH_A observed is used as E^* , the rate constant for rotational transition 1 can be calculated from eq 10 and we obtain

$$k_1 = 1.04 \times 10^{-10} \text{ s}^{-1} \quad \text{at } 20^\circ \text{C} \quad (13)$$

Replacement of \bar{k} in eq 12 with k_1 gives

$$\tau_h = 96 \text{ ps} \quad \text{at } 20^\circ \text{C} \quad (14)$$

This is in complete agreement with the value of 90 ps observed in the present PPO solution.

This result may offer evidence that the relaxation time is explained by Kramers' theory at the low-friction limit and the activation energy represents the barrier height for backbone motion. Correlations among the chain bonds are so limited that associated solvent disturbances are small and viscous friction in the solvent is unimportant.

3. Relaxation of PEO. In the PEO chain, two kinds of rotations are active in dielectric relaxation. One is rotation of an O atom and two H atoms around a C–C bond and the other is that of a CH₂ group around an O–C bond. However, the moment of inertia (0.41×10^{-38} g cm²) is almost the same for these rotations.

The activation energy for PEO of $M = 2.9 \times 10^4$ in benzene obtained from the previous data¹⁶ is 2.1 kcal/mol. Putting these values into eq 11 and 13, we obtain

$$\tau = 26 \text{ ps} \quad \text{at } 20^\circ \text{C} \quad (15)$$

This is also in good agreement with the relaxation time of 17–19 ps observed in this work.

A shorter relaxation time, smaller activation energy, and larger dipole moment ratio (0.73–0.81) for PEO as compared with those for PPO may indicate a smaller restriction of rotation.

4. Effect of Chemical Structure. The relaxation time of PSO in benzene at 20 °C is 350 ps.³⁰ Nevertheless, the activation energy has not been reported previously. If the activation energy is assumed to be the same as that of PPO in benzene, the ratio of the relaxation times observed in polymers agrees with the ratio derived by Kramers' rate constant.

In a PSO chain as in PPO there are four kinds of rotations active in dielectric relaxation. The moment of inertia of rotation of a phenyl group, an O atom, and a H atom around a C–C bond is 12.2×10^{-38} g cm². According to Kramers' theory, the square root of the ratio of the moments of the two polymers gives the ratio of the two relaxation times

$$\tau(\text{PSO})/\tau_h(\text{PPO}) = (I(\text{PSO})/I(\text{PPO}))^{1/2} = 3.7 \quad (\text{calculated}) \quad (16)$$

The ratio of relaxation times obtained experimentally is

$$\tau(\text{PSO})/\tau_h(\text{PPO}) = 350/90 = 3.9 \quad (\text{observed}) \quad (17)$$

In the case of PCL, a relaxation peak was found at 1.9 GHz in dioxane at 25 °C.¹⁷ The ratio of the relaxation time observed

$$\tau(\text{PCL})/\tau_h(\text{PPO}) = 84/74 = 1.1 \quad (\text{observed}) \quad (18)$$

is in good agreement with that calculated

$$\tau(\text{PCL})/\tau_h(\text{PPO}) = 0.9 \quad (\text{calculated}) \quad (19)$$

The effect of chemical structure on the relaxation times is thus explained well by taking into account the moment of inertia of bond rotation in Kramers' rate constant at the low-friction limit.

Registry No. PPO (SRU), 25322-69-4; PEO (SRU), 25322-68-3.

References and Notes

- (1) Stockmayer, W. H. *Pure Appl. Chem.* **1967**, *15*, 539.
- (2) Rouse, P. E. *J. Chem. Phys.* **1953**, *21*, 1272.
- (3) Zimm, B. H. *J. Chem. Phys.* **1956**, *24*, 269.
- (4) Jones, A. A.; Brehm, G. A.; Stockmayer, W. H. *J. Polym. Sci., Polym. Symp.* **1974**, No. 46, 149.
- (5) Bates, T. W.; Ivin, K. J.; Williams, G. *Trans. Faraday Soc.* **1967**, *63*, 1964.
- (6) Matsuo, K.; Mansfield, M. L.; Stockmayer, W. H. *Macromolecules* **1982**, *15*, 935.
- (7) Mashimo, S. *Macromolecules* **1976**, *9*, 91.
- (8) Mashimo, S.; Chiba, A. *Polym. J.* **1973**, *5*, 41.
- (9) Stockmayer, W. H.; Matsuo, K. *Macromolecules* **1972**, *5*, 766.
- (10) Mashimo, S.; Nakamura, H.; Chiba, A. *J. Chem. Phys.* **1982**, *76*, 6342.
- (11) Kramers, H. A. *Physica (Amsterdam)* **1940**, *7*, 284.
- (12) Chandrasekhal, S. *Rev. Mod. Phys.* **1943**, *15*, 1.
- (13) Mashimo, S.; Chiba, A.; Shinohara, K. *Polym. J.* **1974**, *6*, 170.
- (14) Mashimo, S. *J. Chem. Phys.* **1977**, *67*, 2651.
- (15) Mashimo, S.; Winsor, P.; Cole, R. H.; Matsuo, K.; Stockmayer, W. H. *Macromolecules* **1983**, *16*, 965.
- (16) Davies, M.; Williams, G.; Loveluck, G. D. *Z. Elektrochem.* **1960**, *64*, 575.
- (17) Nakamura, H.; Mashimo, S.; Wada, A. *Jpn. J. Appl. Phys.* **1982**, *21*, 1022.
- (18) Iwasa, Y.; Chiba, A. *J. Polym. Sci., Polym. Phys. Ed.* **1977**, *15*, 881.
- (19) Cole, R. H. *J. Phys. Chem.* **1975**, *79*, 1459, 1469.
- (20) Cole, R. H.; Mashimo, S.; Winsor, P. *J. Phys. Chem.* **1980**, *84*, 786.
- (21) Nakamura, H.; Mashimo, S.; Wada, A. *Jpn. J. Appl. Phys.* **1982**, *21*, 467.
- (22) Baur, M. E.; Stockmayer, W. H. *J. Chem. Phys.* **1965**, *43*, 4319.
- (23) Havriliak, S.; Negami, S. *J. Polym. Sci., Part C* **1966**, *14*, 99.
- (24) Abe, A.; Hirano, T.; Tsuji, K.; Tsuruta, T. *Macromolecules* **1979**, *12*, 1100.
- (25) Marchal, J.; Benoit, H. *J. Polym. Sci.* **1957**, *23*, 221.
- (26) Scholtan, W.; Lie, S. Y. *Makromol. Chem.* **1964**, *81*, 14.
- (27) Allen, G.; Booth, A. C.; Jones, M. M. *Polymer* **1964**, *5*, 195.
- (28) Liao, T.-P.; Morawetz, H. *Macromolecules* **1980**, *13*, 1228.
- (29) Volkenstein, M. V. "Configurational Statistics of Polymeric Chains"; Interscience: New York, 1963.
- (30) Matsuo, K.; Stockmayer, W. H.; Mashimo, S. *Macromolecules* **1982**, *15*, 606.

Theory of Potentiometric Titration of Polyelectrolytes: A Discrete-Site Model for Hyaluronic Acid

Robert L. Cleland

Department of Chemistry, Dartmouth College, Hanover, New Hampshire 03755.
Received August 30, 1983

ABSTRACT: The potentiometric titration of weak polyacids which are fully ionized when completely neutralized is treated in terms of a conformation model of the tissue polysaccharide hyaluronic acid, for which the Manning parameter $\xi < 1$. The parameters of the model were chosen to fit approximately the unperturbed Kuhn length and its temperature coefficient. The part of the configurational free energy which depends on the degree of ionization α is the electrostatic free energy, where pair interactions are taken to be given by the simple Debye-Hückel screened Coulomb potential energy. The linear Ising model in the third-nearest-neighbor approximation is used to calculate the titration curve of $\Delta pK = pK_a - pK_0$ as a function of α , where the apparent ionization constant K_a is defined by $pK_a = pH + \log [(1 - \alpha)/\alpha]$ and pK_0 is pK_a for $\alpha = 0$. The average excess free energy (referred to the uncharged state) is shown to be given, to a good approximation for the hyaluronate titration, by an extended Bragg-Williams (EBW) approximation. The resulting approximate titration curve is $\Delta pK/\alpha = (2/2.3kT)(u_1 + u_2 + \dots)$, where u_p is the conformationally averaged excess free energy of interaction of a charged site with its p th nearest neighbor, to be summed over all neighbors. A rough numerical estimate of the sum was obtained from a rigid wormlike ("frozen worm") model for which the pair distances in the Debye-Hückel potential were taken as expansion-corrected unperturbed root-mean-square charge separations, as given by the conformational model. This estimate agreed approximately at several ionic strengths with that obtained from Monte Carlo calculations of the configurational partition function based on the same model. The latter estimate, corrected for the low dielectric constant of the polyion and for salt exclusion by use of a cylinder model, agrees reasonably well with experimental titration data for hyaluronate at low ionic strength I . The corrected result can be approximated at low I by the EBW result for the model of ionization sites spaced equally at distance b on a straight line: $\Delta pK/\alpha = (2\xi/2.3) \ln [1 - \exp(-\kappa b)]$, where κ is the Debye-Hückel screening parameter. The latter result approximates at low I that of the uniformly charged cylinder model with "radius" equal to the site spacing b , which is about 1.0 nm for hyaluronate.

This work concerns the potentiometric titration of the class of polyacids which, even when fully neutralized, are completely ionized (or nearly so) in the Debye-Hückel sense. According to the criterion of Manning,¹ complete ionization occurs for the infinite line charge model of polyelectrolytes when the charge density parameter ξ is less than unity, where ξ is defined by

$$\xi = e^2/DbkT \quad (1)$$

In eq 1, e represents the electronic charge, D the bulk solvent dielectric constant, b the length per unit (electron)

charge, k the Boltzmann constant, and T the absolute temperature. With the bulk dielectric constant $D (=78.3)$ at 25 °C, $\xi = 0.716/b$ (b in nm), so that b must be greater than about 0.7 nm to meet this criterion. As b decreases below this distance, the Manning theory predicts increasing counterion condensation in the near vicinity of the polyion, which partly shields the polyion charge.

As a specific example the present work focuses on the polysaccharide hyaluronic acid, for which experimental titration data are available^{2,3} at several values of the ionic strength I . Hyaluronate, the ionized form of the acid, for